

is discussed in the context of that of the previous paper on (*E*)- and (*Z*)-2,5-dimethylhexatriene, where the corresponding spectra were shown to be different from each other. The present results support the previously discussed validity of the principle of non-equilibration of excited rotamers (NEER) for the triplet states of these molecules in solution. Relative  $E \rightarrow Z$  and  $Z \rightarrow E$  isomerization efficiencies were obtained from ground-state Raman spectra and GC analysis. These indicated a considerably higher  $Z \rightarrow E$  than  $E \rightarrow Z$  efficiency of isomerization from the triplet state, a result suggesting that the minimum of the triplet potential energy surface along the torsional coordinate of the central C=C double bond is shifted toward the planar tEt conformation relative to the maximum of the corresponding ground-state potential energy surface. In the case of a population of various minima in equilibrium on the triplet potential energy surface, the different rates of  $E \rightarrow Z$  and  $Z \rightarrow E$  isomerization suggest at least two minima, one with an essentially planar tEt conformation and the other with a twisted central carbon-carbon bond. Furthermore

the efficiency of conversion of hexatriene to other photoproducts was seen to be larger for *Z*-HT than for *E*-HT. The mechanisms of this formation of photoproducts are not presently known; however, mechanisms not involving the relaxed triplet state of hexatriene must be active. A rather tentative assignment of the resonance Raman spectra of the triplet states of *E*-HT and *Z*-HT, based partly on available calculations in the literature, was attempted.

**Acknowledgment.** We thank A/S Ferrosan for a generous loan of the preparative gas chromatograph, Helge Egsgaard and Ole Jørgensen for invaluable help with the GC apparatus and the purification of samples, and Gert Olsen for help with the excimer laser. We also thank K. B. Hansen for continual support with the development of the experimental facility. This work was partly supported by the Danish National Science Research Council.

**Registry No.** (*Z*)-1,3,5-Hexatriene, 2612-46-6; (*E*)-1,3,5-hexatriene, 821-07-8.

## Electrochemistry and Spectroscopy of Ortho-Metalated Complexes of Ir(III) and Rh(III)

Y. Ohsawa,<sup>†</sup> S. Sprouse,<sup>†</sup> K. A. King,<sup>†</sup> M. K. DeArmond,<sup>†</sup> K. W. Hanck,<sup>†</sup> and R. J. Watts\*<sup>‡</sup>

*Department of Chemistry, North Carolina State University, Raleigh, North Carolina 27695-8204, and*

*Department of Chemistry, University of California, Santa Barbara, California 93106*

*(Received: July 10, 1986; In Final Form: October 8, 1986)*

The electrochemical and UV-visible spectroscopic properties of Rh(III) and Ir(III) complexes of the ortho-metalating (NC) ligands, 2-phenylpyridine (ppy) and benzo[*h*]quinone (bzq), have been studied. Cyclic voltammetric studies of several of the dimeric species,  $[M(\text{NC})_2\text{Cl}]_2$ , indicate metal-centered oxidation occurs at moderate potentials. Cationic monomers of the type  $M(\text{NC})_2(\text{NN})^+$  where (NN) = 2,2'-bipyridine or 1,10-phenanthroline have been prepared by reaction of the chelating ligands with the parent dimers. Cyclic voltammetric studies of these monomers indicate that several reversible ligand-centered reductions are generally observed and that the chelating ligand is more easily reduced than is the ortho-metalating ligand. Spectroscopic studies of the mixed ligand monomers indicate that dual emissions from MLCT states associated with the ortho-metalating and chelating ligands occur in the Ir(III) complexes whereas a single emission from a ligand-localized excited state is observed in the Rh(III) complexes. These results are discussed in terms of electronic and nuclear coupling factors analogous to those encountered in descriptions of bimolecular energy and electron-transfer processes.

### Introduction

The photophysics, photochemistry, and electrochemistry of several  $d^6$  diimine complexes of Ru(II) can be rationalized if the optical and redox orbitals are considered to be localized (spatially isolated orbitals)<sup>1,2</sup> upon a single propellar blade of the tris and bis chelate systems. This model facilitates semiquantitative correlation of optical and electrochemical data.<sup>3</sup> For example, cyclic voltammetric reduction waves<sup>3-5</sup> can be readily associated with a specific ligand in a mixed-ligand complex,  $[\text{RuL}_2\text{L}']^{2+}$ . Further, the ESR method,<sup>6,7</sup> previously used to assess the dynamics of electron hopping in the reduced  $[\text{Ru}(\text{L}^-)\text{L}_2]^+$  species, can in conjunction with electronic spectroscopy<sup>8</sup> and resonance Raman methods<sup>9</sup> produce details of the hopping barrier asymmetry for the mixed ligand complexes.

The isoelectronic  $d^6$  Ir(III) and Rh(III) complexes have been less thoroughly probed than the Ru(II) analogues, no doubt in part due to the more difficult chemistry, but also because of the success of the Ru(II) complexes as photocatalysts. Nevertheless, the mixed-ligand  $[\text{Rh}(\text{bpy})_2(\text{phen})]^{3+}$  and  $[\text{Rh}(\text{phen})_2(\text{bpy})]^{3+}$  species (bpy = 2,2'-bipyridine, phen = 1,10-phenanthroline) were earlier identified<sup>10</sup> as producing a dual  $\pi-\pi^*$  emission of the spatial isolated orbital type, one involving the phen system and the other

the bpy system. Emissions of mixed-ligand analogues derived from the parent  $\text{Ir}(\text{bpy})_3^{3+}$  and  $\text{Ir}(\text{phen})_3^{3+}$  complexes<sup>11-13</sup> might also be expected to show dual emissions, but these would be difficult to prepare and have not yet been reported. Although the photoselection method<sup>14,15</sup> used to identify the spatially isolated

(1) DeArmond, M. K.; Carlin, C. M. *Coord. Chem. Rev.* **1981**, *36*, 325.  
(2) DeArmond, M. K.; Hanck, K. W.; Wertz, D. W. *Coord. Chem. Rev.*, in press.

(3) Ohsawa, Y.; Hanck, K. W.; DeArmond, M. K. *J. Electroanal. Chem.* **1984**, *175*, 229.

(4) Rillema, D. P.; Allen, G.; Meyer, T. J.; Conrad, D. *Inorg. Chem.* **1983**, *22*, 1617.

(5) Morris, D. E.; Ohsawa, Y.; Segers, D. P.; DeArmond, M. K.; Hanck, K. W. *Inorg. Chem.* **1984**, *23*, 3010.

(6) Motten, A. G.; Hanck, K. W.; DeArmond, M. K. *Chem. Phys. Lett.* **1981**, *79*, 541.

(7) Morris, D. E.; Hanck, K. W.; DeArmond, M. K. *J. Am. Chem. Soc.* **1983**, *105*, 3032.

(8) Heath, G. A.; Yellowlees, L. J.; Braterman, P. S. *Chem. Phys. Lett.* **1982**, *92*, 646.

(9) Angel, S. M.; DeArmond, M. K.; Donohoe, R. J.; Hanck, K. W.; Wertz, D. W. *J. Am. Chem. Soc.* **1984**, *106*, 3688.

(10) Halpern, W.; DeArmond, M. K. *J. Lumin.* **1972**, *5*, 225.

(11) Flynn, C.; Demas, J. J. *J. Am. Chem. Soc.* **1974**, *96*, 1959.

(12) Flynn, C.; Demas, J. J. *J. Am. Chem. Soc.* **1975**, *97*, 1988.

(13) Watts, R. J.; Harrington, J.; Van Houten, J. J. *J. Am. Chem. Soc.* **1977**, *99*, 2179.

(14) Fujita, I.; Kobayashi, H. *Inorg. Chem.* **1973**, *12*, 2758.

<sup>†</sup>North Carolina State University.

<sup>‡</sup>University of California.

(localized) orbital emission for  $[\text{Ru}(\text{bpy})_3]^{2+}$  does not give unequivocal evidence<sup>16</sup> for a similar event with  $[\text{Ir}(\text{bpy})_3]^{3+}$  and  $[\text{Ir}(\text{phen})_3]^{3+}$ , the cyclic voltammetry pattern<sup>17,18</sup> does provide some evidence that a similar localization of charge occurs for these Ir(III) and Rh(III) systems.

The diimine complexes of Ir(III) and Rh(III) have high energy emitting states and the M(IV)/M(III) couples for these systems have potentials of +2.5 V (vs. NHE) or greater. These factors effectively preclude use of their excited states in visible light driven photoreduction processes. However, the identification and characterization of ortho-metalated bpy species<sup>19-24</sup> such as  $[\text{Ir}(\text{Hbpy}-\text{C}^2, \text{N}^1)(\text{bpy})_2]^{3+}$  has led to additional focus of effort to characterize the photochemical and photophysical properties of ortho-metalated complexes of Ir(III) and Rh(III) with ligands such as 2-phenylpyridine (ppy) and benzo[*h*]quinoline (bzq). While these ligands are structurally similar to bpy and phen, it has become apparent that the metal-carbon bonds which they form with transition-metal ions impart upon their complexes properties which are quite distinct from those of N-coordinated bpy or phen analogues. The spectroscopic results<sup>25,26</sup> for these materials indicate that ortho-metalation has the effect of raising the energies of ligand field (d-d) excited states to very high levels due to the high position of ppy and bzq in the spectrochemical series. Furthermore, the strong  $\sigma$ -donor abilities of these ligands tends to promote low-energy metal-to-ligand charge-transfer excited states via enhancement of the ease of oxidation at the metal center.<sup>27-30</sup> This combination of effects leads to ortho-metalated complexes which, relative to their N-coordinated bpy and phen analogues, have superior visible light absorption properties and low-energy excited states well-suited to participate in photoredox chemistry. These properties are a direct consequence of the high degree of covalency of the M-C bonds in ortho-metalated complexes, and in this study we have sought to further explore the consequences of the potential high degree of coupling between metal and ligand orbitals in these species. Thus, electrochemical techniques as well as emission spectroscopy have been employed to seek evidence as to whether their redox orbitals can be considered to be spatially isolated, as in several of the N-coordinated species cited above, or whether the high degree of covalency imposes sufficient coupling to lead to fully delocalized molecular energy states.

## Experimental Section

**A. Syntheses and Characterizations.** The mixed-ligand monomers  $[\text{Ir}(\text{ppy})_2(\text{bpy})][\text{PF}_6]$ ,  $[\text{Ir}(\text{bzq})_2(\text{phen})][\text{PF}_6]$ ,  $[\text{Rh}(\text{bzq})_2(\text{phen})][\text{ClO}_4]$ , and  $[\text{Rh}(\text{ppy})_2(\text{bpy})][\text{ClO}_4]$  were prepared by reactions of the appropriate dichloro-bridged dimers<sup>25</sup> of ppy or bzq with bpy or phen. The synthetic procedure used in these

syntheses was a modification of the method employed by Nonoyama<sup>31</sup> for preparation of  $[\text{Rh}(\text{bzq})_2(\text{bpy})]\text{Cl}$ . Detailed procedures are described below. Preparation of  $\text{Ir}(\text{ppy})_3$  is described in a prior publication.<sup>26</sup>

**Bis(2-phenylpyridine-*C*<sup>2</sup>,*N*<sup>1</sup>)(2,2'-bipyridine)rhodium Perchlorate.**  $[\text{Rh}(\text{ppy})_2\text{Cl}]_2$  (50 mg) and 2,2'-bipyridine (20 mg, Mallinckrodt) were dissolved in 15 mL of dichloromethane. To this solution, methanol (15 mL) and saturated aqueous  $\text{NaClO}_4$  (1 mL) were added, and the resulting solution was heated at 35 °C for 2 h. After cooling, addition of water (10 mL) resulted in the formation of a light yellow precipitate which was collected on a glass filter frit. Evaporation of the filtrate to one-half of its original volume resulted in a formation of additional amounts of the yellow precipitate which was collected on a glass filter frit and combined with the initial precipitate to yield a total of 69 mg of the product,  $[\text{Rh}(\text{ppy})_2(\text{bpy})][\text{ClO}_4]$  (92%).

Anal. Calcd for  $\text{RhC}_{32}\text{H}_{24}\text{N}_4\text{ClO}_4$ : C, 57.62%; H, 3.63%; N, 8.40%. Found: C, 56.80%; H, 3.45%; N, 8.05%.

**Bis(benzo[*h*]quinoline-*C*<sup>10</sup>,*N*<sup>1</sup>)(1,10-phenanthroline)rhodium Perchlorate.**  $[\text{Rh}(\text{bzq})_2\text{Cl}]_2$  (50 mg) and 1,10-phenanthroline (20 mg, Mallinckrodt) were dissolved in dichloromethane (10 mL). To this solution, methanol (15 mL) and  $\text{NaClO}_4$  (50 mg) were added. This mixture was heated to 40 °C until the volume was reduced to 15 mL, and water (10 mL) was added, resulting in formation of a yellow precipitate. The precipitate was collected on a glass filter frit and air-dried to give 47 mg of the product,  $[\text{Rh}(\text{bzq})_2(\text{phen})][\text{ClO}_4]$  (62.8%).

Anal. Calcd for  $\text{RhC}_{38}\text{H}_{24}\text{N}_4\text{ClO}_4$ : C, 61.76%; H, 3.28%; N, 7.58%. Found: C, 59.61%; H, 3.45%; N, 7.11%.

**Bis(2-phenylpyridine-*C*<sup>2</sup>,*N*<sup>1</sup>)(2,2'-bipyridine)iridium Hexafluorophosphate.**  $[\text{Ir}(\text{ppy})_2\text{Cl}]_2$  (50 mg) and 2,2'-bipyridine (19 mg) were dissolved in dichloromethane (5 mL) and the solution was stirred for 12 h under nitrogen at ambient temperature. The solvent was then removed on a rotary evaporator and the remaining solids were washed with three portions (10 mL) each of diethyl ether and then hexanes in order to remove excess bipyridine. The crude product was purified by column chromatography on a column of Sephadex LH-20 using ethanol for elution and then by recrystallization from a mixture of dichloromethane and toluene to give 49 mg of  $[\text{Ir}(\text{ppy})_2(\text{bpy})]\text{Cl}$  (75% yield). This was converted to the  $\text{PF}_6$  salt by metathesis with silver hexafluorophosphate in dichloromethane. The complex was characterized by <sup>1</sup>H and <sup>13</sup>C NMR spectroscopies. In <sup>1</sup>H NMR, 12 resonances are observed between 6.2 and 9.8 ppm, consistent with two equivalent sets of four protons each on the two py rings of one bpy and two equivalent sets of eight protons each on the two ppy ligands. Analysis by <sup>13</sup>C NMR using SFORD techniques indicates the presence of four quaternary C atoms, corresponding to the three types of bridging C atoms and the one type of Ir-bonded C atom of the ortho-metalated ppy ligand.

Anal. Calcd for  $\text{IrC}_{32}\text{H}_{24}\text{N}_4\text{Cl}(\text{CH}_2\text{Cl}_2)$ : C, 51.00%; H, 3.37%; N, 7.21%. Found: C, 50.08%; H, 3.52%; N, 7.10%.

**Bis(benzo[*h*]quinoline-*C*<sup>10</sup>,*N*<sup>1</sup>)(1,10-phenanthroline)iridium Hexafluorophosphate.** This complex was prepared in 75% yield from  $[\text{Ir}(\text{bzq})_2\text{Cl}]_2$  and 1,10-phenanthroline by a procedure analogous to the one described above. Characterization of this complex by <sup>1</sup>H NMR spectroscopy indicates that it, like the  $[\text{Ir}(\text{ppy})_2(\text{bpy})]^+$  complex, displays a <sup>1</sup>H NMR spectrum with 12 resonances. SFORD techniques indicate the presence of seven quaternary C atoms in <sup>13</sup>C NMR. These results are consistent with the presence of two symmetrically equivalent ortho-metalated bzq ligands (four types of bridging C atoms and one metalated C atom) and one chelated phen ligand (two types of bridging C atoms) with equivalent halves.

Anal. Calcd for  $\text{IrC}_{38}\text{H}_{24}\text{N}_4\text{Cl}(\text{C}_2\text{H}_5\text{OH})(\text{CH}_2\text{Cl}_2)$ : C, 55.0%; H, 3.60%; N, 6.26%. Found: C, 55.25%; H, 3.62%; N, 6.30%.

**B. Solvents and Chemicals.** Methylene chloride (MC) (Fisher) was distilled over anhydrous  $\text{CaSO}_4$ . Acetonitrile (AN) (Aldrich Gold Label) was vacuum distilled over  $\text{P}_2\text{O}_5$  four times. *N,N*-dimethylformamide (DMF) (Fisher) was dried for several days

- (15) Carlin, C. M.; DeArmond, M. K. *Chem. Phys. Lett.* **1982**, *79*, 541.  
 (16) DeArmond, M. K.; Carlin, C. M.; Huang, W. L. *Inorg. Chem.* **1980**, *19*, 62.  
 (17) Kahl, J.; Hanck, K. W.; DeArmond, M. K. *J. Phys. Chem.* **1978**, *82*, 540.  
 (18) Kew, G.; DeArmond, M. K.; Hanck, K. W. *J. Phys. Chem.* **1974**, *78*, 727.  
 (19) Bergeron, S. F.; Watts, R. J. *J. Am. Chem. Soc.* **1979**, *101*, 3151.  
 (20) Spellane, P. J.; Watts, R. J. *Inorg. Chem.* **1981**, *20*, 3561.  
 (21) Wickramasinghe, W. A.; Bird, P. H.; Serpone, N. J. *J. Chem. Soc., Chem. Commun.* **1981**, 1284.  
 (22) Nord, G.; Hazell, A. C.; Hazell, R. G.; Farver, O. *Inorg. Chem.* **1983**, *22*, 3429.  
 (23) Hazell, A. C.; Hazell, R. G. *Acta. Crystallogr.* **1984**, *C40*, 806.  
 (24) Braterman, P. S.; Heath, G. A.; MacKenzie, A. J.; Noble, B. C.; Peacock, R. D.; Yellowless, L. J. *Inorg. Chem.* **1984**, *23*, 3425.  
 (25) Sprouse, S.; King, K. A.; Spellane, P. J.; Watts, R. J. *J. Am. Chem. Soc.* **1984**, *106*, 6647.  
 (26) King, K. A.; Spellane, P. J.; Watts, R. J. *J. Am. Chem. Soc.* **1985**, *107*, 1431.  
 (27) King, K. A.; Finlayson, M. F.; Spellane, P. J.; Watts, R. J. *Sci. Pap. Inst. Phys. Chem. Res.* **1984**, *78*, 97.  
 (28) Maestri, M.; Sandrini, D.; Balzani, V.; Chassot, L.; Jolliet, P.; Von Zelewsky, A. *Chem. Phys. Lett.* **1985**, *122*, 375.  
 (29) Constable, E. C.; Holmes, J. M. *J. Organomet. Chem.* **1986**, *301*, 203.  
 (30) Reveco, P.; Schmehl, R. H.; Cherry, W. R.; Fronczek, F. R.; Selbin, J. *Inorg. Chem.* **1985**, *24*, 4078.

- (31) Nonoyama, M. *J. Organomet. Chem.* **1974**, *82*, 271.

over molecular sieves (Alfa, Linde AW 500) which had been dried at 150 °C and then mixed with sodium anthracene and allowed to stand for several days to remove trace water and oxygen. In cyclic voltammetric measurements, the dimethylformamide was vacuum distilled into an airtight electrolysis cell containing supporting electrolyte and the complex to be studied immediately prior to use. Methanol (Fisher, Spectranalyzed) and ethanol (Rossville, absolute, Gold Shield) were used in spectroscopic measurements without further purification. Water was first deionized and then distilled from an all-glass Corning megapure still.

Tetraethylammonium hexafluorophosphate (TEAH) was prepared by metathesis of tetraethylammonium chloride and potassium hexafluorophosphate in water, recrystallized from water twice and then from methanol, then vacuum-dried at 140 °C for 1 day. Tetra-*n*-butylammonium hexafluorophosphate (TBAH) was prepared in the same manner as TEAH by using tetra-*n*-butylammonium bromide. The product was recrystallized from ethanol twice and then vacuum-dried at 150 °C for 2 days.

**C. Measurements.** Cyclic voltammetric measurements were made with a PAR 162 potentiostat under nitrogen in a one-compartment electrolysis cell which consisted of a platinum wire working electrode, a platinum wire counter electrode, and a silver wire quasi-reference electrode. The cell and its contents were cooled with a dry ice–2-propanol bath in order to stabilize reduction products sufficiently to observe reversible waves. Ferrocene was added to each sample solution at the end of the measurements, and the ferrocenium/ferrocene ( $\text{Fe}^{+/0}$ ) redox couple was used as an internal potential reference. The half-wave potential of  $\text{Fe}^{+/0}$  in acetonitrile containing 0.1 M TEAH was 0.365 V vs. SSCE at room temperature. This reference potential is less sensitive to solvent and temperature and allows comparison of voltammograms monitored in different solvents and at different temperatures on the same potential scale. All cyclic voltammograms were monitored at scan rates of 1.0 V/s or less and the concentration of the complexes were maintained at 0.5 mM or less.

Emission spectra and excitation spectra were monitored with a Spex Fluorolog photofluorimeter equipped with single monochromators and a Hamamatsu R928 photomultiplier configured for photon counting. Three-dimensional emission intensity/excitation wavelength/emission wavelength contour maps were automatically accumulated with a Spex Datamate under control of an excitation–emission matrix program supplied by Spex Industries, and were plotted on a Houston Instruments Hiplot DMP-3 digital plotter. Emission intensities were ratioed to excitation lamp intensities as monitored by a Rhodamine B quantum counter in order to provide corrected excitation spectral analysis. Emission intensities were corrected for wavelength dependencies of the photomultiplier and optical response characteristics with correction factors generated from a standard quartz–halogen lamp and stored in the Spex Datamate.

Emission lifetimes and time-resolved emission spectra were generated by using an AVCO C950 pulsed nitrogen laser as an excitation source at 337 nm. For measurements at 77 K, samples were placed in 25 mm diameter quartz tubes and submerged in liquid nitrogen in a quartz optical Dewar. Measurements near room temperature were performed on samples in 10-mm rectangular cells which were placed in a thermostated sample holder for temperature control. Emitted light at 90° to the excitation was passed into a Fastie-Ebert 0.8-m scanning grating monochromator with 1-nm optical resolution. Emitted light was detected with an RCA 8852 photomultiplier whose output was applied to the input of either of two computer-controlled boxcar averager systems. One of these systems consisted of a PAR 4422 gated integrator with Model 4420 boxcar averager and 4402 signal processor. The other consisted of Stanford Research Systems SR250 gated integrator with SR280 power supply. This system was interfaced to an IBM PC computer through an SR245 interface using the SR265 data acquisition software. Each of these systems were employed both in a static gate mode for determinations of time-resolved spectra and in scanning gate mode for lifetime determinations.

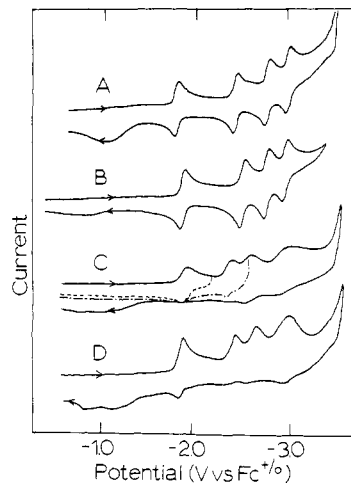


**Figure 1.** Cyclic voltammograms of mixed-ligand complexes in 0.1 M TEAH–dimethylformamide solutions at  $-54$  °C. Scan rate of 0.1 V/s except c where scan rate was 1.0 V/s. (a)  $\text{Ir}(\text{ppy})_2(\text{bpy})^+$ ; (b)  $\text{Rh}(\text{ppy})_2(\text{bpy})^+$ ; (c)  $\text{Rh}(\text{bzq})_2(\text{phen})^+$ ; (d)  $\text{Ir}(\text{bzq})_2(\text{phen})^+$ .

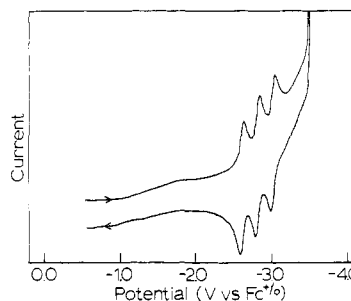


**Figure 2.** Cyclic voltammogram of  $\text{Ir}(\text{ppy})_3$  in 0.1 M TEAP–dimethylformamide at  $-54$  °C. Scan rate of 0.1 V/s.<sup>3</sup>

**TABLE I: Half-Wave Potentials ( $E'_{1/2}$ ) for Monomer Ir(III) and Rh(III) Complexes in Dimethylformamide Containing 0.1 M TEAH at  $-54$  °C**

complex	$E'_{1/2}$ , V vs. $\text{Fc}^{+/0}$				
	2+/ $+$ <sup>a</sup>	+/ $0$	$0/-$	$-2/-$	$2-/3-$
$[\text{Ir}(\text{ppy})_2(\text{bpy})][\text{PF}_6]$	0.86	-1.77	-2.42	-2.77	-3.00
$[\text{Ir}(\text{bzq})_2(\text{phen})][\text{PF}_6]$	0.98 <sup>b</sup>	-1.79	-2.4 <sup>d</sup>	-2.59 <sup>d</sup>	-3.00 <sup>d</sup>
$[\text{Rh}(\text{ppy})_2(\text{bpy})][\text{ClO}_4]$	1.2 <sup>b</sup>	-1.84	-2.49	-2.76	-2.97
$[\text{Rh}(\text{bzq})_2(\text{phen})][\text{ClO}_4]$	1.13 <sup>b</sup>	-1.85 <sup>c</sup>	-2.4 <sup>d</sup>	-2.6 <sup>d</sup>	-2.9 <sup>d</sup>
$[\text{Ir}(\text{ppy})_3]$		0.36	-2.6	-2.8	-3.0

<sup>a</sup> In acetonitrile containing 0.1 M TEAH at  $-40$  °C. <sup>b</sup> Anodic peak potential of irreversible wave. <sup>c</sup> At a scan rate of 1.0 V/s. <sup>d</sup> Highly distorted wave.

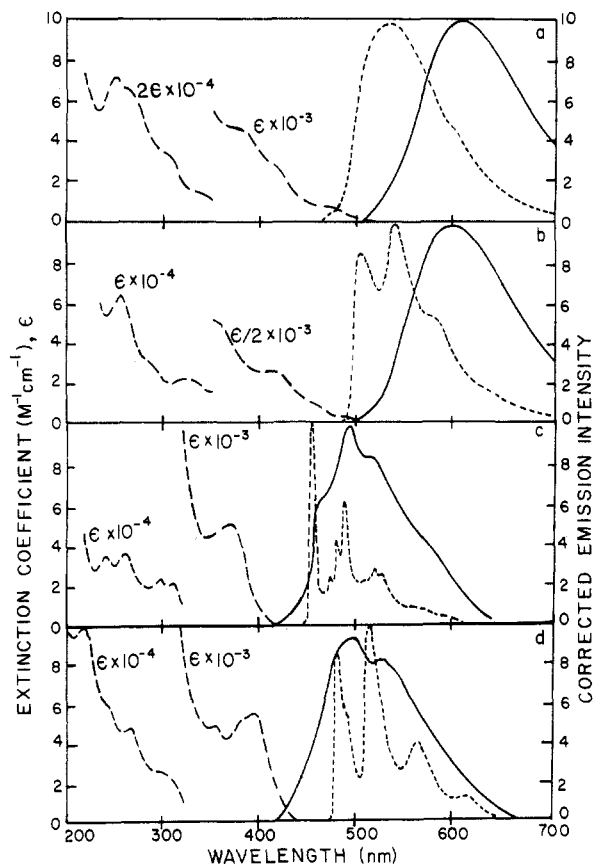
## Results

**A. Electrochemistry.** Figure 1 illustrates cyclic voltammograms for DMF solutions of all four mixed ligand monomers containing 0.1 M TEAH supporting electrolyte at  $-54$  °C. The voltammograms of  $\text{Rh}(\text{bzq})_2(\text{phen})^+$  and  $\text{Ir}(\text{bzq})_2(\text{phen})^+$  were distorted significantly and only the first reduction process was reversible even at a higher scan rate of 1.0 V/s. Both  $\text{Rh}(\text{ppy})_2(\text{bpy})^+$  and  $\text{Ir}(\text{ppy})_2(\text{bpy})^+$  give almost the same redox pattern except for a one-electron reversible oxidation process observed for  $\text{Ir}(\text{ppy})_2(\text{bpy})^+$ . Figure 2 shows the voltammogram for  $\text{Ir}(\text{ppy})_3$  in DMF with 0.1 M TEAP at  $-54$  °C. In addition to the three reversible reduction waves illustrated in Figure 2, a reversible oxidation wave with  $E'_{1/2}$  of 0.36 V vs.  $\text{Fc}^{+/0}$  was observed (Table I). In Table I the half-wave potentials listed are values for waves whose anodic to cathodic peak separation was 50–60 mV, unless otherwise noted. Ohmic loss is likely responsible for deviation from the theoretical value (43 mV); therefore, midpoint potentials were considered to be equal to reversible half-wave potentials. These complexes showed reduction patterns in AN similar to those observed in DMF.

**TABLE II: Cyclic Voltammetric Results for Dichloro-Bridged Dimers of Rh(III) and Ir(III) in Methylene Chloride (MC), Acetonitrile (AN), and *N,N*-Dimethylformamide (DMF)**

complex	base soln	temp, °C	$E_{1/2}^r$ , V vs. $Fc^{+/0}$		
			2+ / +	+ / 0	0 / -
$[Ir(ppy)_2Cl]_2$	MC (0.1 M TBAH)	298	0.77 (90) <sup>a</sup>	0.51 (70) <sup>a</sup>	
$[Ir(ppy)_2Cl]_2$	AN (0.1 M TEAH)	-40		0.61 <sup>b</sup> (60) <sup>a</sup>	-2.4 <sup>c</sup>
$[Ir(ppy)_2Cl]_2$	DMF (0.1 M TEAH)	-54			-2.6 <sup>c</sup>
$[Rh(ppy)_2Cl]_2$	MC (0.1 M TBAH)	298		0.8 <sup>c</sup>	
$[Rh(ppy)_2Cl]_2$	AN (0.1 M TEAH)	-40		0.9 <sup>c</sup>	-2.4 <sup>c</sup>
$[Rh(ppy)_2Cl]_2$	DMF (0.1 M TEAH)	-54		1.3 <sup>c</sup>	-2.6 <sup>c</sup>
$[Ir(bzq)_2Cl]_2$	MC (0.1 M TBAH)	298		0.5 <sup>c</sup>	
$[Ir(bzq)_2Cl]_2$	AN (0.1 M TEAH)	-40		0.6 <sup>c</sup>	-2.3 <sup>c</sup>
$[Ir(bzq)_2Cl]_2$	DMF (0.1 M TEAH)	-54		0.4 <sup>c</sup>	-2.4 <sup>c</sup>

<sup>a</sup>Anodic to cathodic peak separation  $E_p$  in mV. <sup>b</sup>At room temperature 0.58 V vs.  $Fc^{+/0}$ ,  $E_p = 65$  mV. <sup>c</sup>Irreversible wave.



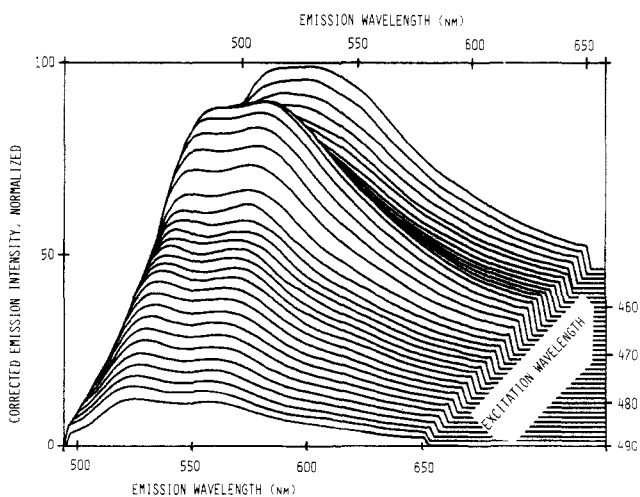
**Figure 3.** Absorption and emission spectra of mixed-ligand complexes: (---) absorption in methanol at room temperature; (---) emission in ethanol-methanol (4:1) at 77 K (—) emission at room temperature in ethanol-methanol (4:1) for Ir(III) complexes and in acetonitrile for Rh(III) complexes. (a)  $Ir(ppy)_2(bpy)^+$ ; (b)  $Ir(bzq)_2(phen)^+$ ; (c)  $Rh(ppy)_2(bpy)^+$ ; (d)  $Rh(bzq)_2(phen)^+$ .

Table II summarizes the available data for the dimer complexes which were studied in three solvents, AN, DMF, and MC. Even with very dry DMF and AN, no reversible reduction wave could be observed. The oxidation of the  $[Ir(ppy)_2Cl]_2$  in MC at room temperature does give two reversible one-electron waves, consistent with the oxidation of the two Ir(III) metal centers, but this same complex in AN at  $-40$  °C gives a single reversible one-electron wave.

**B. Absorption and Emission Spectroscopy.** The absorption spectra of each of the four mixed-ligand monomers at 295 K are presented in Figure 3, and the main features in their absorption spectra are compiled in Table III. The emission spectra of these complexes at 295 and 77 K are also shown in Figure 3. Both Rh(III) complexes as well as the bzq complex of Ir(III) show substantial vibrational structure in their 77 K emission spectra, but this type of structure is absent in the  $Ir(ppy)_2(bpy)^+$  emission. Emissions from the two Ir(III) complexes display large red shifts in fluid solutions at 295 K, whereas the two Rh(III) complexes

**TABLE III: Absorption Features of Ortho-Metalated Ir(III) and Rh(III) Monomers in Methanol**

complex	wavelength, nm	$\epsilon$ , $M^{-1} cm^{-1} \times 10^{-4}$
$Rh(ppy)_2(bpy)^+$	366	0.53
	307	2.3
	296	2.4
	257	3.8
	238	3.7
$Rh(bzq)_2(phen)^+$	393	0.55
	378	0.50
	353	0.49
	333	1.4
	300	2.4
	265	4.7
	242	5.9
$Ir(ppy)_2(bpy)^+$	217	9.9
	206	9.8
	465	0.058
	410	0.28
	375	0.47
$Ir(bzq)_2(phen)^+$	310	1.6
	265	3.2
	252	3.6
	480	0.041
	415	0.51
	325	2.0
	255	6.4



**Figure 4.** Three-dimensional emission intensity/emission wavelength/excitation wavelength spectrum of  $Ir(ppy)_2(bpy)^+$  in ethanol-methanol (4:1) at 77 K.

show only small red shifts with a partial loss of vibrational structure. At 295 K, the two Ir complexes showed strong emissions with measurable lifetimes in hydroxylic solvents such as ethanol, methanol, and water, but emissions from the two Rh monomers could not be observed in these solvents. Weak emissions from the Rh monomers could be observed in non-hydroxylic solvents such as acetonitrile and dichloromethane at 295 K but lifetimes for these emissions were shorter than the time resolution of the

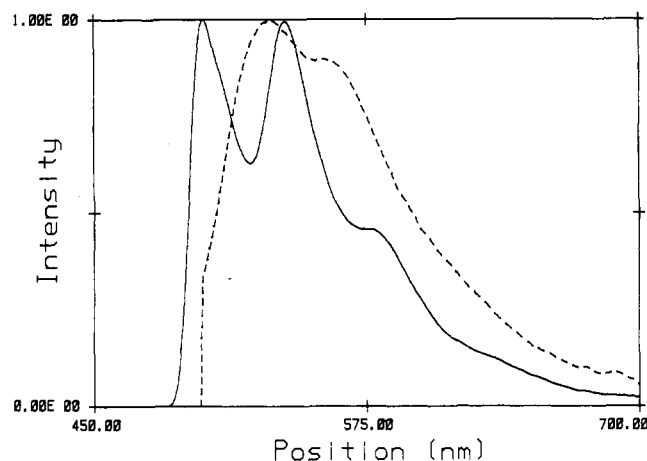


Figure 5. Emission spectra of  $\text{Ir}(\text{bzq})_2(\text{phen})^+$  in ethanol-methanol (4:1) at 77 K excited at 440 nm (—) and at 490 nm (---).

TABLE IV: Emission Energies and Lifetimes of Ortho-Metalated Ir(III) and Rh(III) Monomers

complex	emission energy, <sup>a</sup> $\text{cm}^{-1} \times 10^3$	lifetime, <sup>a</sup> $\mu\text{s}$	emission energy, <sup>b</sup> $\text{cm}^{-1} \times 10^3$	lifetime, <sup>b</sup> $\mu\text{s}$
$\text{Rh}(\text{bpy})_2(\text{bpy})^+$	21.9	177	21.7 <sup>c</sup>	<10 <sup>d</sup>
$\text{Rh}(\text{bzq})_2(\text{phen})^+$	20.7	4250	20.4 <sup>e</sup>	<10 <sup>d</sup>
$\text{Ir}(\text{ppy})_2(\text{bpy})^+$	19.1	4.78	16.5 <sup>f</sup>	0.337 <sup>c</sup>
$\text{Ir}(\text{bzq})_2(\text{phen})^+$	18.6	6.5, <sup>g</sup> 60 <sup>h</sup>	16.8 <sup>f</sup>	0.783 <sup>c</sup>

<sup>a</sup>At 77 K, in ethanol-methanol glass (4:1 by volume), highest energy-resolved peak. <sup>b</sup>At 298 K; highest energy-resolved peak. <sup>c</sup>In degassed acetonitrile. <sup>d</sup>Shorter than pulse of nitrogen laser; in nanoseconds. <sup>e</sup>In degassed dichloromethane. <sup>f</sup>In degassed methanol. <sup>g</sup>Short component of decay described by two exponentials. <sup>h</sup>Long component of decay described by two exponentials.

nitrogen laser (<10 ns). Emission spectra of the four monomers illustrated in Figure 3 were excited at 380 nm, and at 77 K, the shapes of the emission spectra of the two Ir complexes become dependent upon the excitation wavelength when excitation is performed at the long-wavelength edge of the absorption spectrum. This effect is illustrated in Figure 4 with a 3-dimensional emission wavelength/excitation wavelength/emission intensity spectrum of  $\text{Ir}(\text{ppy})_2(\text{bpy})^+$ . The spectrum reveals two resolved features at emission wavelengths of 520 and 550 nm when excitation is carried out at wavelengths longer than 470 nm. At shorter excitation wavelengths, these two features coalesce to a single broad emission centered at about 530 nm. Figure 5 illustrates a comparison of the emission spectra of  $\text{Ir}(\text{bzq})_2(\text{phen})^+$  when excited at 440 nm and at 490 nm. In this case, vibrational structure is observed under both excitation conditions, but the origin red shifts substantially under the longer wavelength excitation. Time-resolved emission spectra of the two Ir monomers display quite distinct effects as illustrated in Figure 6. Whereas  $\text{Ir}(\text{bzq})_2(\text{phen})^+$  displays quite different time components at 100-ns and 50- $\mu\text{s}$  delay times,  $\text{Ir}(\text{ppy})_2(\text{bpy})^+$  displays components at 100 ns and 5  $\mu\text{s}$  which, though different, are less distinct than the components of  $\text{Ir}(\text{bzq})_2(\text{phen})^+$ . This effect is illustrated further in Table IV, in which decay data for these two complexes as a function of emission wavelength is included. The two emission components of  $\text{Ir}(\text{bzq})_2(\text{phen})^+$  have lifetimes which differ by nearly an order of magnitude, whereas single-exponential analysis of  $\text{Ir}(\text{ppy})_2(\text{bpy})^+$  gives sufficiently good data fits so as to suggest that double-exponential analysis cannot give reliable lifetime results. This is taken to indicate that the two emission components of  $\text{Ir}(\text{ppy})_2(\text{bpy})^+$  differ in lifetime by only a very small amount, just within the limits of time-resolved spectral analysis.

## Discussion

A. Cyclic Voltammetry. The cyclic voltammetric results both for the ortho-metalated Rh(III) and Ir(III) dimers (Table II) and for the mixed-ligand monomers (Table I) indicate that the ppy

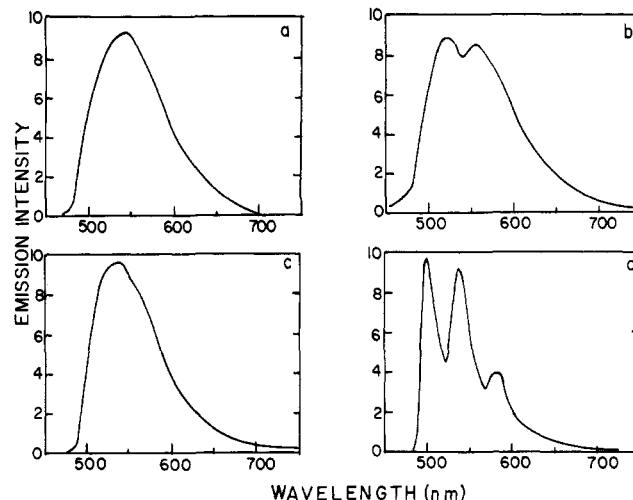


Figure 6. Time-resolved emission spectra of mixed-ligand monomers in ethanol-methanol (4:1) at 77 K. Excited at 336 nm with pulsed nitrogen laser. (a)  $\text{Ir}(\text{ppy})_2(\text{bpy})^+$  at 100 ns after excitation; (b)  $\text{Ir}(\text{ppy})_2(\text{bpy})^+$  at 5  $\mu\text{s}$  after excitation; (c)  $\text{Ir}(\text{bzq})_2(\text{phen})^+$  at 100 ns after excitation; (d)  $\text{Ir}(\text{bzq})_2(\text{phen})^+$  at 50  $\mu\text{s}$  after excitation.

and bzq ligands lead to metal complexes which are more easily oxidized but more difficult to reduce than are similar complexes of bpy or phen. Similar results have been obtained in studies<sup>32,33</sup> of Ru(II) complexes of dipyrildamine as compared to those of bpy. Several lines of evidence suggest that oxidative waves in these ortho-metalated species are due to removal of metal-localized electrons. Of particular significance is the observation of two distinct oxidation waves in MC solutions of  $[\text{Ir}(\text{ppy})_2\text{Cl}]_2$ , attributed to oxidation processes at each of the two metal centers. Prior studies have shown that this complex remains intact as a dimer in MC but is cleaved into solvated monomers in ligating solvents such as AN. This type of cleavage appears to be consistent with the observation of a single reduction wave in AN solutions of the complex. Additional evidence in support of metal-centered oxidations is found in comparisons of the positions of the first oxidation waves of  $\text{Ir}(\text{ppy})_2(\text{bpy})^+$  and of  $\text{Ir}(\text{ppy})_3$ . The position of this wave is shifted cathodically by 0.84 V in the latter complex. Since bpy is known to be difficult to oxidize and ppy oxidation is unlikely to depend upon the number of ppy ligands, this large cathodic shift is consistent with a metal-centered process. The high position of ppy and bzq in the spectrochemical series is indicative of the strong  $\sigma$ -donor qualities imparted by the metal-carbon bonds in conjunction with  $\pi$ -acceptor abilities associated with the heterocyclic portions of the ligand. It is apparently this  $\sigma$ -donor ability associated with metal-carbon bonding which renders the metal centers electron-rich and facilitates oxidation at the metal in  $\text{Ir}(\text{ppy})_3$  relative to  $\text{Ir}(\text{ppy})_2(\text{bpy})^+$ .

The pattern of reduction waves observed in the four mixed-ligand monomers as well as in  $\text{Ir}(\text{ppy})_3$  indicates a process associated not only with ligand-localized acceptor orbitals, but with acceptor orbitals which are localized on the pyridine rings of these ligands. Thus, each of the mixed ligand monomers displays a similar pattern of four reduction waves regardless of whether the metal center is Ir(III) or Rh(III). This strongly supports assignment of these waves to reduction at each of the pyridine rings present in the complex. In each case this pattern consists of one wave at about -1.8 V vs.  $\text{Fc}^{+/0}$  separated from a series of three other waves by about 0.9 V. These three remaining waves occur at similar potentials in each of the complexes, and are separated from each other by potentials of about 0.2-0.3 V. Comparison of the reduction waves in  $\text{Ir}(\text{ppy})_3$  with the mixed-ligand monomers reveals that this complex displays only three waves which are

(32) Morris, D. E.; Ohsawa, Y.; Segers, D. P.; DeArmond, M. K.; Hanck, K. W. *Inorg. Chem.* **1984**, *23*, 3010.

(33) Segers, D. P.; DeArmond, M. K. *J. Phys. Chem.* **1982**, *86*, 3768.

(34) Barigelletti, F.; Belser, P.; von Zelewsky, A.; Juris, A.; Balzani, V. *J. Phys. Chem.* **1985**, *89*, 3680.

separated from one another by about 0.2 V and correspond closely to the three most cathodically shifted waves of the mixed-ligand monomers. Finally, prior cyclic voltammetric studies<sup>17</sup> of Ir(bpy)<sub>3</sub><sup>3+</sup> have shown that a series of six reduction waves occur in two groups of three waves. As in the ortho-metalated species reported here, waves within each group are separated by about 0.2–0.3 V, and the two groups are separated by a larger gap of about 0.7 V. This pattern of six waves has been attributed to a series of three one-electron reductions at each of the three neutral bpy ligands, followed by a second series of three one-electron reductions at each of the previously reduced bpy ligands. The total of six waves corresponds to the number of pyridine rings present in the complex. Since Ir(ppy)<sub>2</sub>(bpy)<sup>+</sup> contains only a single bpy ligand, the pattern of a single reduction wave followed by a group of three reduction waves suggests that the single wave is due to reduction of the bpy moiety, and the group of three waves is associated with reductions at the previously reduced bpy and the two ppy ligands. Similarly, the pattern of three reduction waves observed in Ir(ppy)<sub>3</sub> is thought to be associated with reductions at each of the three pyridine rings of the ppy ligands. In this interpretation, phenyl rings of ppy, which are formally treated as anionic moieties, are regarded much like reduced pyridine rings and are not subject to further reduction. The number of unreduced pyridine rings correlates with the number of reduction waves observed in cyclic voltammetry of each of the complexes discussed above. The reduction waves observed in Ir(bzq)<sub>2</sub>(phen)<sup>+</sup> and in Rh(bzq)<sub>2</sub>(phen)<sup>+</sup> are distorted, but occur at potentials similar to one another and to the Ir(ppy)<sub>2</sub>(bpy)<sup>+</sup> and Rh(ppy)<sub>2</sub>(bpy)<sup>+</sup> complexes. An interpretation of the reductive cyclic voltammetry analogous to that offered for the ppy complexes above appears to be appropriate.

The cyclic voltammetric results for the dichloro-bridged dimers indicate that all of these undergo irreversible reductions in MC solutions. This is probably due to cleavage of the dimers into monomers as the reducing electron is added to the already-electron-rich species. In this context, it is significant that the dimers are formed in preference to monomeric dichloro species in the reaction of Ir(III) with ppy, a fact which may be taken as an indication of the electron-rich nature of the metal centers which leads to sharing of anionic Cl<sup>-</sup> ligands through bridging in order to reduce the negative charge density which would be imposed by two terminal Cl<sup>-</sup> ligands in a monomer.

**B. Emission Spectroscopy.** The emission spectra of the Rh(III) monomers presented in Figure 3 are quite similar to those which were reported previously for the parent dimers, [Rh(ppy)<sub>2</sub>Cl]<sub>2</sub> and [Rh(bzq)<sub>2</sub>Cl]<sub>2</sub>. As was noted in that case, these emissions occur at wavelengths close to the π–π\* phosphorescence of uncomplexed ppy and bzq, and the dimer emissions were assigned as ligand-localized transitions of the metalated ppy and bzq ligands. Analogous π–π\* assignments are applicable to the Rh(ppy)<sub>2</sub>(bpy)<sup>+</sup> and Rh(bzq)<sub>2</sub>(phen)<sup>+</sup> monomer emissions presented here. These assignments are supported by the lifetimes of the Rh(III) monomer emissions reported in Table IV. These are similar to those reported previously for their parent dimers (93 μs for [Rh(ppy)<sub>2</sub>Cl]<sub>2</sub> and 2700 μs for [Rh(bzq)<sub>2</sub>Cl]<sub>2</sub>) and are of a magnitude consistent with this assignment. Finally, the emissions in fluid solutions, though weak, show only small red shifts relative to those displayed in glasses at 77 K. Recent reports of similarly small shifts in other metal complexes displaying π–π\* emissions lend further support to the assignments.<sup>34</sup>

Evidence for dual emissions from Ir(ppy)<sub>2</sub>(bpy)<sup>+</sup> and from Ir(bzq)<sub>2</sub>(phen)<sup>+</sup> in 77 K glasses is apparent in the time-resolved spectra of these presented in Figure 6. Two potential sources of dual emissions which are considered here include impurity emissions from a mixture of cis and trans geometric isomers and intrinsic dual emissions due to slow energy transfer between excited states. Several types of evidence suggest that this dual emission behavior is not due to a cis–trans isomer mixture or to other types of impurities. Samples of both Ir(III) complexes were purified by column chromatography on Sephadex LH-20, and were isolated as single bands from elution. No evidence for an isomer mixture or other impurities was found in either <sup>1</sup>H or <sup>13</sup>C NMR spec-

troscopy. Although the NMR analysis does not provide sufficient evidence to identify which structural isomer is formed, several factors strongly favor a preferred cis disposition of Ir–C bonds. Firstly, a body of structural evidence exists which suggests that the cis geometry is generally favored over a trans arrangement of metal–carbon bonds in ortho-metalated species.<sup>35–37</sup> Secondly, recent X-ray crystal structure determinations of both [Rh(ppy)<sub>2</sub>Cl]<sub>2</sub> and [Ir(ppy)<sub>2</sub>Cl]<sub>2</sub> (ppy = *p*-tolylpyridine) indicate that metal–carbon bonds are cis to one another in these parent dimers.<sup>38</sup> The relatively mild conditions under which the monomers are formed from these dimers suggest that retention of the cis geometry is favored in formation of the monomers. As a result, we conclude that the dual emission behavior observed in these complexes arises from an intrinsic property of the cis isomers.

Due to this added complexity, assignments of emissions from the two Ir(III) monomers are considered separately. The substantial difference in the lifetimes of the two emissions of Ir(bzq)<sub>2</sub>(phen)<sup>+</sup> facilitates good resolution of the longer lived component. Its energy and structure are quite similar to those reported for [Ir(bzq)<sub>2</sub>Cl]<sub>2</sub>; however, the lifetime of the longer component (60 μs) exceeds that reported for the parent dimer (30 μs). It is also significant that the structure observed in the π–π\* emission of [Rh(bzq)<sub>2</sub>Cl]<sub>2</sub> is similar to that seen in the MLCT emission of [Ir(bzq)<sub>2</sub>Cl]<sub>2</sub>, and the Ir complex emission is at only modestly longer wavelength than the Rh complex emission. These factors suggest the longer lived component of the Ir(bzq)<sub>2</sub>(phen)<sup>+</sup> emission is probably due to an excited state which is appropriately described as an admixture of MLCT and π–π\* contributions. Although the exact orbital origin of this emission may not lend to its classification as either π–π\* or MLCT, it is significant that the longer component seems clearly to be associated with the bzq portion of the mixed-ligand complex.

The shape of the emission from the shorter lived component is not apparent in the short delay (100 ns) spectrum of Figure 6, which is a summation of both components. However, some insight into the shape of its emission spectrum may be found in Figure 5, which illustrates the effect of excitation wavelength on the time-integrated emission spectrum. The wavelengths of the maxima in this spectrum excited at 440 nm are identical with those in the long-delay spectrum while the maxima shift to longer wavelengths and are less clearly resolved under 490-nm excitation. Superposition of the components excited at 440 and 490 nm could clearly lead to the structureless emission observed at short delay times (Figure 6). As a result, the spectrum excited at 490 nm in Figure 5 is thought to be that of the component with a lifetime of 6.5 μs in the double-exponential decay analysis. This lifetime and the structured emission suggest a MLCT excited state. Further evidence in support of this assignment is found in the room temperature emission spectrum in Figure 3b. The large red shift in this spectrum relative to the 77 K spectrum is indicative of the MLCT nature of this emission, as is the 295 K lifetime (Table IV). Assignment of which ligand is the electron acceptor in the formation of this excited state can be deduced from the cyclic voltammetric results, which, according to the discussion presented above, indicate that phen is the site of the first reduction wave. Consequently, the 6.5 μs component of the emission is assigned as a MLCT localized in the Ir–phen portion of the molecular framework.

The similarity in emission lifetimes of the two component emissions of Ir(ppy)<sub>2</sub>(bpy)<sup>+</sup> renders time-resolved analysis of this species far more difficult than is the case for Ir(bzq)<sub>2</sub>(phen)<sup>+</sup>. However, some indication of a component with a structured emission is evident in the long-delay spectrum in Figure 6b, which displays poorly resolved bands at about 520 and 550 nm. These same two bands are evident in the three-dimensional spectrum

(35) Hoare, R. J.; Mills, O. S. *J. Chem. Soc., Dalton Trans.* **1972**, 2138.

(36) Chassot, L.; Muller, E.; von Zelewsky, A. *Inorg. Chem.* **1984**, *23*, 4249.

(37) Vicente, J.; Chicote, M. T.; Bermudez, M. O.; Solans, X.; Font-Altaba, M. *J. Chem. Soc., Dalton Trans.* **1984**, 557.

(38) Garces, F.; Watts, R. J., unpublished results.

in Figure 4 when excitation is carried out at wavelengths in excess of 470 nm. Thus, both the time-resolved spectrum in Figure 6b and the excitation-wavelength resolved spectrum in Figure 4 appear to be capable of partially resolving the structure of one of the two components in the emission of  $\text{Ir}(\text{ppy})_2(\text{bpy})^+$ . The second component, which apparently has a slightly shorter lifetime and absorbs at shorter wavelengths, is unresolved in each of the two experimental methods. The magnitude of the lifetime observed in the decay of this complex as well as the vibrational structure of the longer lived component suggest a MLCT assignment to this component. This assignment is supported by the large red shift observed in the 295 K emission spectrum relative to the 77 K emission, illustrated in Figure 2. It is again likely that the coordinating bpy ligand, which cyclic voltammetry suggests to be the better electron acceptor, is the ligand to which this MLCT occurs. The similarity in the lifetime of the second component to the first would suggest that a second MLCT excited state may be responsible for this emission. Its apparent higher energy would be consistent with a MLCT to the ppy ligand in accordance with our interpretation of the cyclic voltammetric results.

### Summary and Conclusions

The cyclic voltammetric results for the ortho-metalated ppy and bzq complexes studied here indicate that they are far more easily oxidized than their bpy or phen counterparts and that this oxidation appears to occur at the metal center. The number of reduction waves corresponds to the number of pyridine rings in the ligands, and NN-coordinating ligands such as bpy or phen contain pyridine rings which are more easily reduced than those contained in NC-metalating ligands such as ppy and bzq.

Emission results indicate that the Rh(III) monomers display low-temperature luminescence from  $\pi-\pi^*$  excited states while the corresponding Ir(III) monomers generally display MLCT luminescence spectra at low temperatures. It is somewhat surprising to find that no indications of dual emissions have been found in either  $\text{Rh}(\text{ppy})_2(\text{bpy})^+$  or in  $\text{Rh}(\text{bzq})_2(\text{phen})^+$  while both  $\text{Ir}(\text{ppy})_2(\text{bpy})^+$  and  $\text{Ir}(\text{bzq})_2(\text{phen})^+$  are characterized by emissions from two nonequilibrated states at 77 K. The first examples of dual emissions from metal complexes were in mixed bpy-phen complexes of Rh(III), which display nonequilibrated  $\pi-\pi^*$  emissions centered on both the bpy and phen ligands.<sup>39-41</sup> Although evidence for a similar behavior in  $\text{Rh}(\text{ppy})_2(\text{bpy})^+$  and in  $\text{Rh}(\text{bzq})_2(\text{phen})^+$  has been sought by both time-resolved techniques and by variations in excitation wavelength, no evidence for dual emissions has thus far been found. The close similarity in both the structure and the energy of the emission spectra of these complexes with those of the parent dimers indicates that both  $\pi-\pi^*$  emissions are localized on the ortho-metalated ppy or bzq ligand. The  $\pi-\pi^*$  emission of bzq coordinated to Rh(III) is substantially lower in energy than that of phen coordinated to Rh(III), and this may lead to an energy gap between these two states in  $\text{Rh}(\text{bzq})_2(\text{phen})^+$  which is adequate to ensure sufficient coupling to establish thermal equilibration of the two. This type of behavior has been observed<sup>41</sup> in complexes such as  $\text{Rh}(\text{bpy})_2(5,6\text{-mephen})^{3+}$  where energy gaps between  $\pi-\pi^*$  states of bpy and 5,6-mephen are similar to those between phen and bzq. However, the energy of the  $\pi-\pi^*$  emission of ortho-metalated ppy in  $\text{Rh}(\text{ppy})_2(\text{bpy})^+$  is quite similar to the energy for the  $\pi-\pi^*$  emission of coordinated bpy in complexes such as  $\text{Rh}(\text{bpy})_3^{3+}$ . In spite of this similarity in energetics of the  $\pi-\pi^*$  states of bpy and ppy, the equilibration of these states in  $\text{Rh}(\text{ppy})_2(\text{bpy})^+$  is quite distinct from the dual emission behavior of complexes such as  $\text{Rh}(\text{bpy})_2(\text{phen})^+$ . This equilibration of the  $\pi-\pi^*$  states of bpy and ppy in  $\text{Rh}(\text{ppy})_2(\text{bpy})^+$  is attributed to a strong electronic coupling of these states through the Rh-C bonds which does not occur through the Rh-N bonds in complexes such as  $\text{Rh}(\text{bpy})_2(\text{phen})^+$ .

Since this coupling must occur through the Rh(III) center, it is significant that a relatively low-energy MLCT absorption band was reported for  $[\text{Rh}(\text{ppy})_2\text{Cl}]_2$ , and a similar absorption feature appears at 366 nm in  $\text{Rh}(\text{ppy})_2(\text{bpy})^+$  with an extinction coefficient of  $5300 \text{ M}^{-1} \text{ cm}^{-1}$  (Figure 3). A similar absorption band appears at 393 nm with an extinction coefficient of  $5500 \text{ M}^{-1} \text{ cm}^{-1}$  in  $\text{Rh}(\text{bzq})_2(\text{phen})^+$ , but no similar absorption features occur in  $\text{Rh}(\text{bpy})_3^{3+}$ ,  $\text{Rh}(\text{phen})_3^{3+}$ , or their mixed bpy-phen derivatives. A MLCT assignment of this band is further supported by the dependence of its position upon solvent. This type of low-energy MLCT is expected to involve the bpy or phen ligand in  $\text{Rh}(\text{ppy})_2(\text{bpy})^+$  and  $\text{Rh}(\text{bzq})_2(\text{phen})^+$ , and may provide a mechanism for electronic coupling of the higher energy  $\pi-\pi^*$  state of coordinated bpy with the  $\pi-\pi^*$  state of coordinated ppy. Treatment of the transfer of energy from a  $\pi-\pi^*$  state of bpy to a  $\pi-\pi^*$  state of ppy can be described in a manner analogous to bimolecular exchange energy transfer.<sup>42,43</sup> In this formalism, essential electronic coupling of these states requires two distinct types of orbital overlap. These are the direct interaction of the LUMO  $\pi^*$  orbitals of bpy and ppy and the indirect interaction of HOMO  $\pi$  orbitals of these ligands through the  $d(\pi)$  Rh(III) orbitals. Energy transfer between  $\pi-\pi^*$  excited states of bpy and phen in complexes such as  $\text{Rh}(\text{bpy})_2(\text{phen})^{3+}$  would, on the other hand, not be assisted by a high-energy  $d(\pi)\text{Rh}$  orbital. As a result, direct coupling of the LUMO  $\pi^*$  orbitals of bpy and phen as well as their HOMO  $\pi$  orbitals would be required. The added spatial extension of LUMO  $\pi^*$  orbitals relative to HOMO  $\pi$  orbitals suggest that the  $\pi^*-\pi^*$  interaction required in both types of complexes will be larger than the  $\pi-\pi$  interaction needed for energy transfer in the bpy-phen complexes. This limited direct interaction between the HOMO  $\pi$  orbitals of bpy and of phen is presumably an important factor in the dual emission behavior in mixed bpy-phen Rh(III) complexes. The indirect interaction of  $\pi(\text{bpy})$  and  $\pi(\text{ppy})$  orbitals through an intervening  $d(\pi)$  Rh(III) orbital associated with the low-energy MLCT state in  $\text{Rh}(\text{ppy})_2(\text{bpy})^+$  could supplant the direct  $\pi-\pi$  interaction described above and account for the enhanced energy transfer between its  $\pi-\pi^*$  excited states relative to those of mixed bpy-phen complexes of Rh(III).

The dual emission behavior of  $\text{Ir}(\text{ppy})_2(\text{bpy})^+$  and  $\text{Ir}(\text{bzq})_2(\text{phen})^+$  is in sharp contrast to the results discussed above for the analogous Rh(III) complexes. In each of the Ir(III) species the observed dual emissions are consistent with two nonequilibrated MLCT states and the lower of these appears to involve the NN-coordinated bpy or phen ligand whereas the higher one appears to involve the NC-metalated ligand. This is an unanticipated result which seems to suggest that even the highly covalent bonding of Ir to C in these species does not assure sufficient coupling of excited states to bring about their thermal equilibration in glasses at 77 K. This coupling is analogous to the type of coupling encountered in intervalence electron transfer,<sup>44</sup> which can occur indirectly by interaction of the  $\pi^*$  orbitals of bpy and of ppy with the  $d(\pi)$  orbitals of Ir, or by a direct interaction of the  $\pi^*$  orbitals of bpy and ppy. Either of these interactions could be as large or larger than those for coupling of the  $\pi-\pi^*$  states of bpy and ppy in  $\text{Rh}(\text{ppy})_2(\text{bpy})^+$ , where two types of orbital overlaps are required. Therefore, it is unreasonable to expect that the dual emissions of these Ir(III) complexes result from the absence of adequate electronic coupling. Rather, this may indicate that the nuclear distortions in these two types of MLCT excited states are sufficiently large to provide a viscosity-dependent Franck-Condon barrier which prohibits energy transfer from one MLCT state to the other.<sup>45,46</sup> The existence of such a barrier is consistent with the large red shifts observed for the MLCT Ir(III) complex

(42) Turro, N. J. *Modern Molecular Photochemistry*; W. A. Benjamin: Menlo Park, CA, 1978.

(43) Balzani, V.; Bolletta, F.; Scandola, F. *J. Am. Chem. Soc.* **1980**, *102*, 2152 and references therein.

(44) Meyer, T. J. *Acc. Chem. Res.* **1978**, *11*, 94 and references therein.

(45) Dellinger, B.; Kasha, M. *Chem. Phys. Lett.* **1975**, *36*, 410; **1976**, *38*, 9.

(46) Watts, R. J.; Missimer, D. *J. Am. Chem. Soc.* **1978**, *100*, 5350.

(39) Halper, W.; DeArmond, M. K. *J. Lumin.* **1972**, *5*, 225.

(40) Crosby, G. A.; Elfring, W. H. Jr. *J. Phys. Chem.* **1976**, *80*, 2206.

(41) Watts, R. J.; Van Houten, J. *J. Am. Chem. Soc.* **1978**, *100*, 1718.

emissions between 77 and 295 K, in contrast to the small red shifts observed for the  $\pi$ - $\pi^*$  emissions of analogous Rh(III) complexes. This type of nuclear barrier may be sufficiently important in ortho-metalated Ir(III) complexes to prohibit thermal equilibration of their close-lying MLCT excited states even though the electronic coupling of these states is promoted by their Ir-C bonds. In fact, these same Ir-C bonds may, through trans effects, be responsible for distortions which give rise to barriers. The nature of the nuclear distortions in which these barriers originate is presently under investigation.

**Acknowledgment.** This work was supported by the Office of Basic Energy Sciences, United States Department of Energy, Project DE-AT03-78ER70277 (University of California at Santa Barbara), and by the National Science Foundation Grant CHE-8507801 (North Carolina State University).

**Registry No.** bpy, 366-18-7; phen, 66-71-7; [Ir(ppy)<sub>2</sub>(bpy)][PF<sub>6</sub>], 106294-60-4; [Ir(bzq)<sub>2</sub>(phen)][PF<sub>6</sub>], 106294-61-5; [Rh(ppy)<sub>2</sub>(bpy)][ClO<sub>4</sub>], 106251-21-2; [Rh(bzq)<sub>2</sub>(phen)][ClO<sub>4</sub>], 106251-23-4; [Rh(ppy)<sub>2</sub>Cl]<sub>2</sub>, 33915-80-9; [Rh(bzq)<sub>2</sub>Cl]<sub>2</sub>, 33915-76-3; [Ir(ppy)<sub>2</sub>Cl]<sub>2</sub>, 92220-65-0; [Ir(bzq)<sub>2</sub>Cl]<sub>2</sub>, 52352-02-0; [Ir(ppy)<sub>3</sub>], 94928-86-6.

## Solid-State Oxygen-17 Nuclear Magnetic Resonance Spectroscopic Studies of Alkaline Earth Metasilicates

Hye Kyung C. Timken,<sup>†</sup> Suzanne E. Schramm,<sup>†§</sup> R. James Kirkpatrick,<sup>‡</sup> and Eric Oldfield<sup>\*†</sup>

School of Chemical Sciences and Department of Geology, University of Illinois at Urbana—Champaign, Urbana, Illinois 61801 (Received: August 1, 1986)

We have obtained high-field (11.7 T, 67.8 MHz) <sup>17</sup>O nuclear magnetic resonance (NMR) spectra of a series of alkaline earth metasilicates (clinoenstatite, MgSiO<sub>3</sub>; diopside, CaMgSi<sub>2</sub>O<sub>6</sub>; pseudowollastonite,  $\alpha$ -CaSiO<sub>3</sub>; strontium metasilicate,  $\alpha$ -SrSiO<sub>3</sub>; and barium metasilicate, BaSiO<sub>3</sub>). Values of the nuclear quadrupole coupling constants ( $e^2qQ/h$ ), electric field gradient tensor asymmetry parameters ( $\eta$ ), and isotropic chemical shifts ( $\delta_i$ ) have been deduced for all the types of oxygen sites encountered. The  $e^2qQ/h$  values for the nonbridging oxygens (Si-O-M, M = divalent cation) are in the range 1.6–3.2 MHz and increase with increasing cation electronegativity, the asymmetry parameters vary from 0 to 0.1, and the isotropic chemical shifts become more deshielded with increasing cation radius. The total range of isotropic chemical shifts for the nonbridging oxygens is 127 ppm. For the bridging oxygens (Si-O-Si) in the metasilicates, the  $e^2qQ/h$  values are in the range from 3.7 to 5.1 MHz and the asymmetry parameters vary from 0.2 to 0.4. The isotropic chemical shifts again become more deshielded with increasing cation radius, the total range of isotropic chemical shifts being 25 ppm. The chemical shifts for both bridging and nonbridging oxygens in metasilicates indicate that deshielding may be correlated with the presence of large cations, as found previously for <sup>17</sup>O NMR spectra of the group IIA (2) and group IIB (12) oxides.

### Introduction

Oxygen is a major constituent of all silicates and of many organic polymers, so <sup>17</sup>O solid-state nuclear magnetic resonance (NMR) spectroscopy should have considerable potential for investigating the structures of such materials.<sup>1-3</sup> In this paper, we present the first comprehensive report of the solid-state <sup>17</sup>O NMR spectra of a series of alkaline earth metasilicates (diopside, CaMgSi<sub>2</sub>O<sub>6</sub>; clinoenstatite, MgSiO<sub>3</sub>; pseudowollastonite,  $\alpha$ -CaSiO<sub>3</sub>; strontium metasilicate,  $\alpha$ -SrSiO<sub>3</sub>; and barium metasilicate, BaSiO<sub>3</sub>), using high-field (11.7 T, 67.8 MHz and 8.45 T, 48.8 MHz) NMR of <sup>17</sup>O labeled materials.

### Experimental Section

**Synthetic Aspects.** All the silicates were synthesized by using Si<sup>17</sup>O<sub>2</sub> (prepared from the hydrolysis of SiCl<sub>4</sub> with 40 atom % H<sub>2</sub>[<sup>17</sup>O]) (vide infra), obtained from Cambridge Isotope Laboratories, Cambridge, MA) and high-purity metal carbonates, MCO<sub>3</sub> (M = Ca, Sr, or Ba), or MgO. Oxygen-17-enriched SiO<sub>2</sub> was synthesized by dissolving 3.40 g of SiCl<sub>4</sub> in 30 mL of anhydrous diethyl ether under an N<sub>2</sub> atmosphere and then syringing in 1.3 mL of 40 atom % H<sub>2</sub>[<sup>17</sup>O] to cause hydrolysis of the SiCl<sub>4</sub>, basically as outlined by Bray et al.<sup>2</sup> A 1.43-g yield of enriched silica gel was thus obtained. The silica gel was then fired either at 1500 °C for about 15 min or at 350 °C for about 24 h to drive off volatile impurities. X-ray diffraction analyses indicated the SiO<sub>2</sub> to be amorphous after the 350 °C calcination or in the form of low cristobalite after the high-temperature calcination. Alkaline-earth-containing silicate glasses were then prepared with

99.999% metal carbonates (or MgO) and <sup>17</sup>O-enriched silica. Each glass was melted at about 50 °C above its *liquidus* and then quenched and ground to a fine powder. The process was repeated three times. To minimize loss of <sup>17</sup>O to the atmosphere, the enriched glasses were fused for only about 20 min each time. Crystalline metasilicates were finally obtained by crystallization of the isochemical glass at temperatures some 50–100 °C below the *solidus*. Purities were verified by means of powder X-ray diffraction.

**Spectroscopic Aspects.** Oxygen-17 NMR spectra were recorded at 67.8 and 48.8 MHz with "home-built" spectrometers. These consist of 11.7-T, 52-mm-bore or 8.45-T, 89-mm-bore superconducting solenoids (Oxford Instruments, Osney Mead, U.K.), Nicolet (Madison, WI) Model 1280 data acquisition systems, Amplifier Research (Souderton, PA) Model 200L amplifiers (for radio-frequency pulse generation), and "home-built" static (solenoidal) and "magic-angle"<sup>4</sup> sample-spinning (MASS) probes. The solution 90° pulse widths were in the range of 15–20  $\mu$ s, and 5–7  $\mu$ s pulses were used for data acquisition on the solid samples (where only the  $1/2$ ,  $-1/2$  transition is observed, for both bridging and nonbridging oxygens). Typical recycle times of 30–120 s were used, based on preliminary recycle time dependencies of the <sup>17</sup>O NMR spectra. The spectra were simulated as described elsewhere.<sup>5</sup> All the chemical shifts are quoted with respect to the <sup>17</sup>O NMR signal of external tap water at 25 °C, with high-fre-

(1) Oldfield, E.; Kirkpatrick, R. J. *Science* **1985**, *227*, 1537.

(2) Bray, P. J.; Bucholtz, F.; Geissberger, A. E.; Harris, I. A. *Nucl. Instrum. Methods* **1982**, *199*, 1.

(3) Schramm, S. E.; Kirkpatrick, R. J.; Oldfield, E. *J. Am. Chem. Soc.* **1983**, *105*, 2483.

(4) Andrew, E. R. *Progress in Nuclear Magnetic Resonance Spectroscopy*; Emsley, J. W., et al., Eds.; Pergamon: New York, 1971.

(5) Ganapathy, S.; Schramm, S. E.; Oldfield, E. *J. Chem. Phys.* **1982**, *77*, 4360.

<sup>†</sup>School of Chemical Sciences.

<sup>‡</sup>Department of Geology.

<sup>§</sup>Present address: Mobil Research and Development Corporation, P.O. Box 1025, Princeton, NJ 08540.